A Model-Based Approach for Voltage and State-of-Charge Estimation of Lithium-ion Batteries

Milad Andalibi
University of Zagreb, Faculty of Electrical Engineering and Computing, Department of Control and Computer Engineering
Zagreb, Croatia
milad.andalibi@fer hr

Seyed Saeed Madani
Institute of Applied Materials-Applied Materials Physics, Karlsruhe Institute of Technology
Karlsruhe, Germany
seyed madani@kit.edu

Carlos Ziebert
Institute of Applied Materials-Applied Materials Physics, Karlsruhe Institute of Technology
Karlsruhe, Germany
carlos.ziebert@kit.edu

Farshid Naseri
Aarhus University
Electrical Energy Technology, Electrical and Computer Engineering Department
Aarhus, Denmark
fna@ece.au.dk

Mojtaba Hajihosseini
University of Zagreb Faculty of Electrical Engineering and Computing, Laboratory for Renewable Energy Systems
Zagreb, Croatia
Mhajihosseini@fer.hr

***Abstract*— Electric vehicles are equipped with a large number of lithium-ion battery cells. To achieve superior performance and guarantee safety and longevity, there is a fundamental requirement for a Battery Management System (BMS). In the BMS, accurate prediction of the State-of-Charge (SOC) is a crucial task. The SOC information is needed for monitoring, controlling, and protecting the battery, e.g. to avoid hazardous over-charging or over-discharging. Nonetheless, the SOC is an internal cell variable and cannot be straightforwardly obtained. This paper presents a Kalman Filter (KF) approach based on an optimized second-order Rc equivalent circuit model to carefully account for model parameter changes. An effective machine learning technique based on Proximal Policy Optimization (PPO) is applied to train the algorithm. The results confirm the high robustness of the proposed method to varying operating conditions.**

Keywords*— *Energy Storage System, State-of-Charge (SOC), extended Kalman Filter (EKF), Electric Vehicle (EV)

I. Introduction

Today, due to the large number of cars and the increase in the consumption of fossil fuels in them and, consequently, the increase in air pollution, the question arises as to how long the environment can withstand these conditions. Transportation electrification is an effective way to cut down pollution caused by the mobility sector. In this pathway, Lithium-ion (Li-ion) batteries play a crucial role. The battery pack in Electric Vehicles (Evs) is composed of a large number of cells that are operated based on the Battery Management System (BMS). To effectively control and protect the batteries, it is essential to estimate their State-of-Charge (SoC) in the BMS. The information will be subsequently used to operate the battery within the safe charge limits, predict the driving range, etc. Various methods have been presented for estimating the battery SOC. Coulomb counting [1-3] is one of the simplest techniques, where SOC is computed by integrating the measured current. Another simple approach is the open-circuit voltage (OCV) technique, where the SOC is calculated using the OCV-SOC relation [4-6]. However, these methods are unsuitable because error accumulation in the Coulomb counting method results in inaccurate SOC estimation, and the OCV technique is ineffective when EV is in use because the battery must be disconnected from the circuit to let it rest. Impedance spectroscopy is also used to determine the SOC of the battery by correlating the recorded impedances of the battery at different SOC values [7]. However, this technique is time-consuming and temperature-dependent in addition to being offline. It also requires additional laboratory testing, which drives up the cost. Neural Networks (NNs) [8-10], Kalman filter (KF), and KF extensions for nonlinear systems such as the extended Kalman filter (EKF) and the sigma-point KF (SPKF) are other techniques for SOC estimation which outperform the traditional techniques [11-19].

The EKF technique, unlike classical estimation methods of SOC (such as the ampere-hour integration method), does not rely on the initial value of SOC and has no accumulated error, making it ideal for actual EV operating conditions. EKF is a model-based method, and thus, the prediction error of the SOC is highly dependent on the accuracy of the battery model and model parameters. The characteristics of Li-ion batteries change due to a variety of factors and indicate considerable nonlinearity and variance over time. The battery is approximated as a linear, time-invariant system in a typical EKF technique; however, this approach presents estimation errors [11-19]. So far, a set of methods for measuring or estimating SOC is presented, which is summarized in [20]. Among these methods, a number have been used, such as the KF-based methods in BMS.

To eliminate the aforementioned problems and improve SOC estimation accuracy, this paper presents an estimation technique that integrates time-varying battery parameters into the EKF algorithm. The proposed method is based on the Proximal Policy Optimization (PPO) to carefully optimize the model in the EKF algorithm for SOC estimation.

II. Battery Modeling

Fig.1 depicts a second-order RC equivalent circuit model (ECM) of a Li-ion battery. Voltages, resistors, and capacitors are employed in the model. The polarization response of the battery is represented by RC structures. The terminal voltage, measured directly at either end, is denoted by U_L.

$$\begin{bmatrix} V_1{}' \\ V_2{}' \end{bmatrix} = \begin{bmatrix} -\frac{1}{R_1 C_1} & 0 \\ 0 & -\frac{1}{R_2 C_2} \end{bmatrix} \begin{bmatrix} V_1 \\ V_2 \end{bmatrix} + I \begin{bmatrix} \frac{1}{C_p} \\ \frac{1}{C_e} \end{bmatrix} \tag{1}$$

V_1 and V_2 denote the cell polarization voltages, respectively; V_1' denotes the first derivative of V_1; V_2' denotes the first

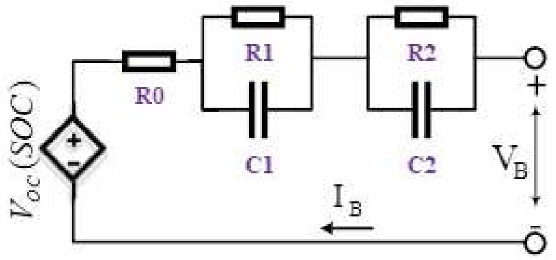

Fig. 1. Second-order RC ECM of the Li-ion battery

derivative of V_2; and $[V_1 \quad V_2]^T$ denotes the state variable. The output equation of the model is:

$$U_L = U_{oc} - V_1 - V_2 - IR_0 \tag{2}$$

III. SOC AND EXTENDED KALMAN FILTER

A summary of EKF in SOC estimation is shown in Fig. 2. A nonlinear system and the observation model can be described by the state space as:

$$X_k = f(X_{k-1}) + W_{k-1} \tag{3}$$

$$Z_k = h(X_k) + V_k \tag{4}$$

X_k is the system's state vector with n dynamic variables, while $f(\cdot)$ and $h(\cdot)$ are nonlinear vector functions that represent the system and observation, respectively. Process and measurement noises are represented by W_k and V_k, while observation error is specified by Z_k.

The system has a random initial state X_0 with the mean and covariance of μ_0 and P_0 with the definition of:

$$\mu_0 = E[X_0] \tag{5}$$

$$P_0 = E[(X_0 - \mu_0)(X_0 - \mu_0)^T] \tag{6}$$

where $E[X_0]$ shows the expected value operator and the term T represents the transforming factor. W_k and V_k are uncorrelated white noises and so, $E[W_k] = 0$, $E[V_k] = 0$, and $E\left[W_k V_j^T\right] = 0$ for all k and j. The covariance matrices are defined as $Q_k = E\left[W_k W_k^T\right]$ and $R_k = E\left[V_k V_k^T\right]$. With the only available information on the mean and the covariance of the initial state, the first optimal state estimation would be $X_0^a = \mu_0 = E[X_0]$. By continuing iteratively, optimal estimates as $X_{k-1}^a = E[X_{k-1}|Z_{k-1}]$ with the covariance of P_{k-1} the following states would be obtained as:

$$X_k^f = E[f(X_{k-1})|Z_{k-1}] \tag{7}$$

$f(\cdot)$ can be approximated by Taylor Series expansion about the X_{k-1} point:

$$f(X_{k-1}) \equiv f(X_{k-1}^a) + \mathcal{J}_f(X_{k-1}^a)(X_{k-1} - X_{k-1}^a) + \mathrm{H.O.T.} \tag{8}$$

where $\mathcal{J}_f$ is the Jacobian of $f(\cdot)$, and H.O.T denotes the higher-order terms. Considering negligible H.O.T. and the definition of $e_{k-1} = X_{k-1} - X_{k-1}^a$, (8) can be rewritten as:

$$f(X_{k-1}) \approx f(X_{k-1}^a) + \mathcal{J}_f(X_{k-1}^a)e_{k-1} \tag{9}$$

Considering (9), applying the expected value on (10), and that $E[e_{k-1}|Z_{k-1}] = 0$, then the forecast state X_k^f, the error e_k^f, and covariance P_k^f would be estimated as follows:

$$X_k^f \approx f(X_{k-1}^a) \tag{10}$$

$$\begin{aligned} e_k^f &\equiv X_k - X_k^f \\ &= f(X_{k-1}) + W_{k-1} - f(X_{k-1}^a) \\ &\approx \mathcal{J}_f(X_{k-1}^a)e_{k-1} + W_{k-1} \end{aligned} \tag{11}$$

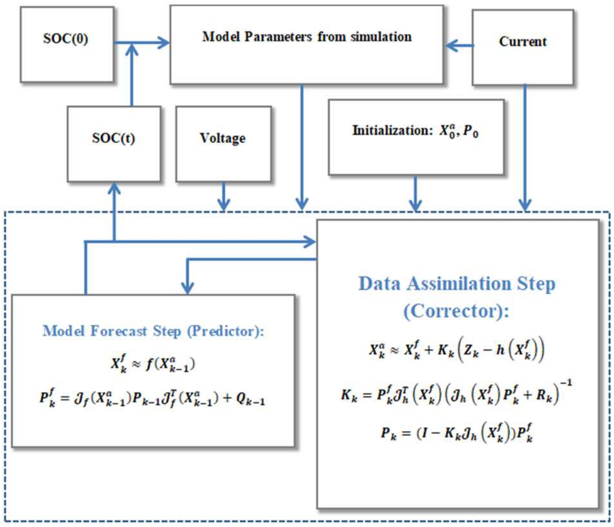

Fig. 2. EKF in SOC estimation scheme

$$\begin{aligned} P_k^f &\equiv E\left[e_k^f\left(e_k^f\right)^T\right] \\ &= \mathcal{J}_f(X_{k-1}^a)E\left[e_{k-1}^f\left(e_{k-1}^f\right)^T\right]\mathcal{J}_f^T(X_{k-1}^a) \\ &\quad + E\left[W_{k-1}W_{k-1}^T\right] \\ &= \mathcal{J}_f(X_{k-1}^a)P_{k-1}\mathcal{J}_f^T(X_{k-1}^a) + Q_{k-1} \end{aligned} \tag{12}$$

A linear equation of X_k^a and Z_k to estimate the states:

$$X_k^a = a + K_k Z_k \tag{13}$$

To obtain the parameter a, the following term should provide the condition of unbiasedness:

$$\begin{aligned} &E[X_k - X_k^a|Z_k] = \\ &= E\left[\left(X_k^f + e_k^f\right) - (a + K_k h(X_k) + K_k V_k)|Z_k\right] \\ &= X_k^f - a - K_k E[h(X_k)|Z_k] \end{aligned} \tag{14}$$

$$a = X_k^f - K_k E[h(X_k)|Z_k] \tag{15}$$

Substituting a from (15) in (13) would be $X_k^a = X_k^f + K_k(Z_k - E[h(X_k)|Z_k])$. Expanding $h(\cdot)$ in Taylor Series about x_k^f using the same methods as in the model forecast phase yields:

$$h(X_k) \equiv h\left(X_k^f\right) + \mathcal{J}_f\left(X_k^f\right)\left(X_k - X_k^f\right) + \mathrm{H.O.T.} \tag{16}$$

Using (16) and applying the expected value to (17), and assuming $E[e_k^f|Z_k)] = 0$, the forecast state X_k^a, error e_k, and posterior covariance P_k are calculated as follows:

$$X_k^a \approx X_k^f + K_k\left(Z_k - h\left(X_k^f\right)\right) \tag{17}$$

$$\begin{aligned} e_k &\equiv X_k - X_k^a \\ &\approx \left(I - K_k J_h\left(X_k^f\right)\right)\mathcal{J}_f(X_{k-1}^a)e_{k-1} + \Big(I - \\ &\quad K_k J_h\left(X_k^f\right)\Big)W_{k-1} - K_k V_k \end{aligned} \tag{18}$$

$$\begin{aligned} P_k &\equiv E\left[e_k e_k^T\right] \\ &= P_k^f - K_k\mathcal{J}_h\left(X_k^f\right)P_k^f - P_k^f\mathcal{J}_h^T\left(X_k^f\right)K_k^T \\ &\quad + K_k\mathcal{J}_h\left(X_k^f\right)P_k^f\mathcal{J}_h^T\left(X_k^f\right)K_k^T \\ &\quad + K_k R_k K_k^T \end{aligned} \tag{19}$$

Kalman gain is obtained as follows by optimizing (20) with respect to K_k.

$$K_k = P_k^f\mathcal{J}_h^T\left(X_k^f\right)\left(\mathcal{J}_h\left(X_k^f\right)P_k^f + R_k\right)^{-1} \tag{20}$$

P_k would then be rewritten as:

$$P_k = (I - K_k\mathcal{J}_h\left(X_k^f\right))P_k^f \tag{21}$$

IV. PROXIMAL POLICY-BASED OPTIMIZATION

In the Reinforcement Learning (RL) context, tasks are defined using a quintuple $\{S, A, r, p, \gamma\}$, where $S \in \mathbb{R}^n$ represents the states space, $A \in \mathbb{R}^m$ represents the action space, $r: S \times A \to \mathbb{R}$ represents the function of reward, $p: S \times A \times S \to [0,1]$ represents the transition function that determines the transfer probability of a new state s_{t+1}, resulting a reward r under execution. The RL aims to optimize the acquired rewards $\mathbb{E}[\sum_{t=0}^{\infty} \gamma^t r_t]$ using the starting state s_t, which is a random set.

PPO (Proximal Policy Optimization) acts on an MDP (Mixed Distributed Proximal) environment by following an optimum policy. In many scenarios, the hyper parameters of the PPO converge very fast.

The primary objective of policy gradient techniques is to decrease the variation of gradient estimations, resulting in more consistent progress. The Actor-Critic architecture has a substantial influence on this approach since it represents a new definition of value function:

$$Q^\pi(s,a) = \sum_t \mathbb{E}_{\pi_\theta}[R(s_t,a_t)|s.a] \tag{22}$$

$$V^\pi(s) = \sum_t \mathbb{E}_{\pi_\theta}[R(s_t,a_t)|s] \tag{23}$$

$$A^\pi(s,a) = Q^\pi(s,a) - V^\pi(s) \tag{24}$$

The advantage function $A^\pi(s,a)$ determines how advantageous an action is in comparison to the other options accessible in a given condition. $V(s)$ is a value function that determines how nice it is to be in that state. By evaluating the cumulative receiving rewards, the Critic network is trained to anticipate the value function. As one of the most effective Actor-Critical techniques, the PPO seeks to maximize the objective function, which is expressed as follows:

$$L(\theta) = \hat{\mathbb{E}}_t[\min(r_t(\theta)\hat{A}_t, clip(r_t(\theta), 1-\epsilon, 1+\epsilon)\hat{A}_t)] \tag{25}$$

in which A and E are, respectively, the advantage function and expectation estimations and $r_t(\theta)$ is the ratio of probability formulated as:

$$r_t(\theta) = \frac{\pi_\theta(a_t,s_t)}{\pi_{\theta_{old}}(a_t,s_t)} \tag{26}$$

Vanilla policy gradients need instances of optimized policymaking which are inapplicable to the changed policy upon every optimization cycle. Significance of sampling is used by PPO to determine the samples' expected number from a previous policy under the next policy. Every single sample may be utilized for many gradient ascent steps for this purpose. Whenever the next policy is modified, the previous and next policies diverge, causing the estimation variance to grow. The previous policy will also be changed to the next policy. A comparable function for state transition must exist to fulfil this aim, which herein is guaranteed by dividing the ratio of probability to the area $[1-\epsilon, 1+\epsilon]$.

V. PPO-BASED BATTERY MODEL PARAMETER TUNER

The PPO technique is considered in this paper as a mechanism to adaptively tune and update the RC model's parameters by utilising the RL's real-time learning and model-independency properties. The R_0, R_1, R_2, C_1 and C_2 are regarded as the design deciding parameters' objectives in the proposed approach, and the tuning algorithm modifies the values by real-time learning of the NNs. Fig. 3 shows the suggested ULM adaptive controller based on the PPO tuner.

The PPO generates the commands $[dR_0(t)\ dR_1(t)\ dR_2(t)\ dC_1(t)\ dC_2(t)]$ to modify the values using the Actor and Critic NNs, as shown in Fig. 3. As these parameters are generally non-zero, the updating parameters structure is constructed as follows:

$$R_i(t+1) = R_i(t) + dR_i(t),\ \ i = 0,1,2$$

$$C_j(t+1) = C_j(t) + dC_j(t),\ \ j = 1,2$$

The PPO agent seeks to decrease the error between the calculated battery voltage in the RC model and its real value from the applied data sets by training the coefficients of Actor and Critic NNs. The current from data set I, the battery's output voltage v_o, the error e of v_o, and the battery voltage

$$J(\theta) = \mathbb{E}_{\mathcal{T}\sim\pi_\theta(\tau)}\left[\sum_t R(s_t,a_t)\right] = \mathbb{E}_{\mathcal{T}\sim\pi_\theta(\tau)}[R(\tau)] \tag{27}$$

$$\nabla_\theta J(\theta) = \mathbb{E}_{\mathcal{T}\sim\pi_\theta(\tau)}\left[\left(\sum_{t=1}^{T} \nabla_\theta \log\pi_\theta(a_t|s_t) R(\tau)\right]\right. \tag{28}$$

from data set v_{data} $(e = v_o - v_{data})$ and their derivation e and v_o, i.e. $state = \left\{I, v_o, \left(\frac{dv_o}{dt}\right), e, \left(\frac{de}{dt}\right)\right\}$. In order to make up the output voltage, PPO algorithm's reward function r_t is adjusted to:

$$r_t = -e_t^2 \tag{29}$$

The Critic and Actor NNs are created with four completely connected HLs with 50 neurons. For all HLs in the NNs, the mapping function is considered to be nonlinear and based on the rectified linear unit (ReLU). Detailed list of the algorithmic parameters including the PPO and NNs (as configured in Fig. 4) are provided in Table I.

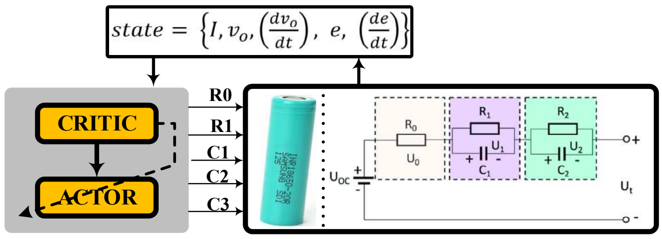

Fig. 3. The ULM controller according to the PPO tuning

TABLE I
THE SETTINGS OF THE PPO

Parameter	Value	Parameter	Value
Length of training episode in PPO	1800 ts	Factor of discount	0.9
Size of batch	1024 eps	Rate of learning	0.001
Rate of learning in Actor	0.008	MC cycles	1000
Rate of learning in Critic	0.008		

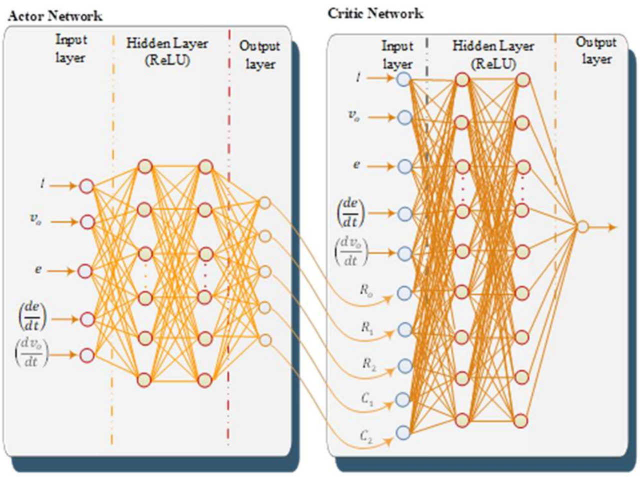

Fig. 4. Configuring the PPO algorithm and the NNs

VI. Results and Discussions

To determine the battery parameters, the model values of RC networks are determined experimentally under different SOC and C rates. The parameter identification results are entered into a lookup table, and in the EKF system matrix, the battery parameters are updated by matching the values in the table. Moreover, using the error analysis to estimate the charge level, one also obtains an estimate of the nonlinear part of the battery model, and by adding this nonlinear part to the linear model, one obtains a more accurate model of the battery. The accuracy of the SOC, which is estimated using this approach, is direct and depends on the precision of the battery model and model parameters.

One of the KF requirements is to know the covariance noise matrices of measurement and process. Nonetheless, the covariance matrices are difficult to obtain in real life. In case of incorrect tuning of Q and R matrices, the filter's performance is affected, the accuracy of estimating the charge status is reduced, and the filter could diverge. To address this issue, the performance of the KF estimator is monitored through a designed algorithm. Accordingly, the algorithm adjusts the covariance matrices R and Q such that the filter achieves a good performance.

The proposed model and the EKF-based SOC estimation technique are implemented, and the model parameters were experimentally obtained by considering various SOC and C-rates. The following steps were then taken:

1. The outcomes of the parameter identification were entered into a lookup table,
2. In the EKF system matrix, the battery parameters are updated by matching the values in the table;
3. Estimate the charge level using the error analysis;
4. Obtains an estimate of the nonlinear part of the battery model;
5. Adding the nonlinear part to the linear model;

To validate the presented method, the experimental data obtained through various validation tests based on DST and US06 were applied. The tests were performed at two SOC levels, including 0.5 and 0.8, and three discharge pulses were investigated for each SOC condition. At three test temperatures 0°C, 25°C, and 45°C the tests were iterated. Fig. 5 shows the estimated SOC using EKF with the time-varying model parameters at 0°C, 25°C, and 45°C for the three experimental data, i.e., DST and US06. The outcomes indicate that the estimations of SOC in each temperature are accurate. A comparison of the estimation results with the actual results shows the efficiency of the proposed method in estimating the charge level of cells and, thus, the actual charge level of a battery pack. In Fig. 5, the predicted voltage is compared to the observed voltage. With less than a 30 mV discrepancy, it is reasonable to assume that the real and predicted voltage are well matched.

It is compared to conventional techniques to assess the accuracy of the suggested approach. The results confirm the effectiveness of the suggested algorithm compared to the existing techniques. As the results show, the estimation error of the SOC in all conditions remains low with the proposed method, while the prediction error with other techniques increases when the statistical features of the covariance matrices are unknown.

The process and measurement noise are known, and unknown statistical characteristics remain low. In contrast, when the statistical characteristics of process noise and measurement are unknown, accuracy is reduced in other methods.

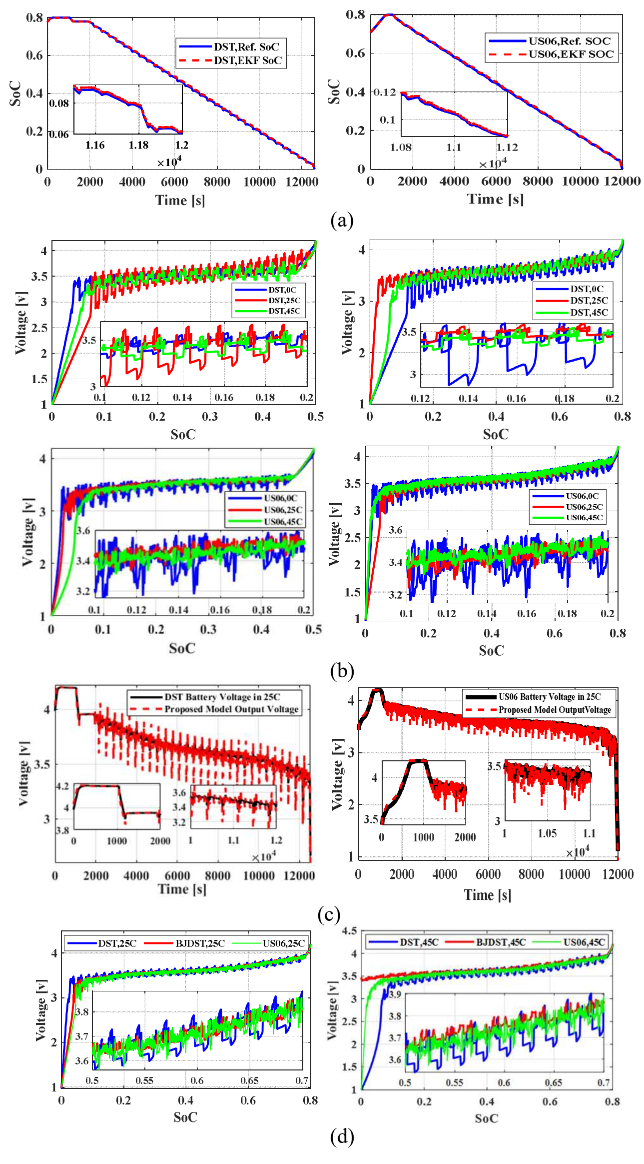

Fig. 5. (a) comparison of the real SOC and EKF estimation at 25°C tested under DSTC and US06C. (b) tests of the SOC at 25°C and 45°C at 0.5 SOC for the data of DSTC and US06C. (c) comparison of the real voltage and the model voltage of the data of DSTC and US06C. (d) the obtained voltage at 0.8 SOC at 0°C, 25°C, and 45°C for the data of DSTC and US06C.

The results confirm that the SOC estimation is robust in different operating conditions, including different C-rates and temperature conditions. Likewise, the SOC estimation error in the low-SOC region is relatively lower than the conventional methods.

VII. Conclusion

In this paper, the KF algorithm is presented to improve the SOC estimation accuracy in EVs. Although the proposed method has a higher computational burden compared to classical SOC estimators, the SOC estimation accuracy considering the initial error, is improved. In addition, the results show that in situations where the assumptions and initial information are unknown, the performance of the model does not change when the information is correctly available, thus providing optimal performance for the system. The proposed method is validated using experimental data of a typical Li-ion battery cell. The results of experimental tests indicate the proper performance of the proposed method in estimating the battery SOC.

References

[1] 1.Awadallah MA, Venkatesh B (2016) Accuracy improvement of state of charge estimation in lithium-ion batteries. J Energy Storage 6: 95–104.

[2] 2. Leksono E, Haq IN, Iqbal M, et al. (2013) STATE OF CHARGE (soc) estimation on lifepo4 battery module using coulomb counting methods with modified peukert. 2013 Joint International Conference on Rural Information Communication Technology and Electric-Vehicle Technology (rICT & ICeV-T) 2013.

[3] 3. Jeong YM, Cho YK, Ahn JH, et al. (2014) Enhanced coulomb counting method with adaptive state of charge reset time for estimating ocv. 2014 IEEE Energy Conversion Congress and Exposition 1313–1318.

[4] 4. Lipu MH, Hannan M, Hussain A, et al. (2018) A review of state of health and remaining useful life estimation methods for lithium-ion battery in electric vehicles: Challenges and recommendations. J Cleaner Prod 2018.

[5] 5. Deng Y, Hu Y, Cao Y (2014) An improved algorithm of state of charge testing based on opencircuit voltage-ampere hour method. International Conference on Life System Modeling and Simulation and International Conference on Intelligent Computing for Sustainable Energy and Environment 258–267.

[6] 6. Murnane M, Ghazel A (2017) A closer look at STATE OF CHARGE (soc) and state of health (soh) estimation techniques for batteries. Available from: http://www.analog. com/media/en/technical-documentation/technicalarticles/A-Closer-Look-at-State- Of-Charge-and-State-Health-Estimation-Techniques-.... pdf.

[7] 7. State-of-health monitoring of lithium-ion batteries in electric vehicles by on-board internal resistance estimation, Journal of Power Sources 196 (2011) 5357–5363.

[8] 8. He W, Williard N, Chen C, et al. (2014) STATE OF CHARGE estimation for li-ion batteries using neural network modeling and unscented kalman filter-based error cancellation. Int J Electr Power Energy Syst 62: 783–791.

[9] 9. Wu J, Zhang C, Chen Z (2016) An online method for lithium-ion battery remaining useful life estimation using importance sampling and neural networks. Appl energy 173: 134–140.

[10] 10. Liu F, Liu T, Fu Y (2015) An improved state of charge estimation algorithm based on artificial neural network. 2015 8th International Symposium on Computational Intelligence and Design(ISCID) 2: 152–155.

[11] 11. Jiang C, Taylor A, Duan C, et al. (2013) Extended kalman filter based battery STATE OF CHARGE (soc) estimation for electric vehicles. 2013 IEEE Transportation Electrification Conference and Expo (ITEC) 2013: 1–5.

[12] 12. Topan PA, Ramadan MN, Fathoni G, et al. (2016) STATE OF CHARGE (soc) and state of health (soh) estimation on lithium polymer battery via kalman filter. International Conference on Science and Technology-Computer (ICST) 2016: 93–96.

[13] 13. Zhang S, Sun H, Lyu C (2018) A method of state of charge estimation for power li-ion batteries based on equivalent circuit model and extended kalman filter. 2018 13th IEEE Conference on Industrial Electronics and Applications (ICIEA) 2018: 2683–2687.

[14] 14. Sangwan V, Kumar R, Rathore AK (2017) State-of-charge estimation for li-ion battery using extended kalman filter (ekf) and central difference kalman filter (cdkf). 2017 IEEE Industry Applications Society Annual Meeting 2017: 1–6.

[15] 15. Yang Y, Cui N, Wang C,et al. (2017) State of charge estimation of lithium-ion battery based on new adaptive fading extended kalman filter. Chinese Automation Congress (CAC). 2017: 5630–5634.

[16] 16. Liu Z, Wang Y, Du J, et al. (2012) Rbf network-aided adaptive unscented kalman filter for lithium-ion battery state of charge estimation in electric vehicles. 2012 7th IEEE Conference on Industrial Electronics and Applications (ICIEA). 2012: 1673–1677.

[17] 17. Yang D, Liu J, Wang Y, et al. (2014) State-of-charge estimation using a self-adaptive noise extended kalman filter for lithium batteries. 2014 IEEE PES Asia-Pacific Power and Energy Engineering Conference (APPEEC). 2014: 1–5.

[18] 18. Xing Y, He W, Pecht M, et al. (2014) STATE OF CHARGE estimation of lithium-ion batteries using the open-circuit voltage at various ambient temperatures. Appl Energy 113: 106–115.

[19] 19. Rahul K, Ramprabhakar J, Shankar S (2017) Comparative study on modeling and estimation of STATE OF CHARGE in battery. 2017 International Conference On Smart Technologies For Smart Nation (SmartTechCon). 2017: 1610–1615.

[20] 20. M.A. Hannana,, M.S.H. Lipu, A. Hussain, A. Mohamed, A review of lithium-ion battery STATE OF CHARGE estimation and management system in electric vehicle applications: Challenges and recommendations, Renewable and Sustainable Energy Reviews,Volume 78, October 2017, Pages 834-854.